Geophysical Research Letters

RESEARCH LETTER
10.1029/2023GL103773

Key Points:

- The simulated ozone tendency due to chemistry is of the same order of magnitude but of the opposite sign than that due to dynamics
- The chemistry-driven change in the tropical ozone tendency is dominated by the gas-phase rather than heterogeneous chemistry
- The ozone tendency change due to heterogeneous chemistry is saturated when the injected SO_2 amount exceeds 2 Tg

Supporting Information:

Supporting Information may be found in the online version of this article.

Correspondence to:

P. Yu and W. Tian,
pengfei.yu@colorado.edu;
wstian@lzu.edu.cn

Citation:

Peng, Y., Yu, P., Portmann, R. W., Rosenlof, K. H., Zhang, J., Liu, C.-C., et al. (2023). Perturbation of tropical stratospheric ozone through homogeneous and heterogeneous chemistry due to Pinatubo. *Geophysical Research Letters*, *50*, e2023GL103773. https://doi.org/10.1029/2023GL103773

Received 20 MAR 2023
Accepted 25 JUN 2023

Perturbation of Tropical Stratospheric Ozone Through Homogeneous and Heterogeneous Chemistry Due To Pinatubo

Yifeng Peng[1], Pengfei Yu[2], Robert W. Portmann[3], Karen H. Rosenlof[3], Jiankai Zhang[1], Cheng-Cheng Liu[4], Jiangtao Li[1], and Wenshou Tian[1]

[1]College of Atmospheric Sciences, Lanzhou University, Lanzhou, China, [2]Institute for Environmental and Climate Research, Jinan University, Guangzhou, China, [3]Chemical Science Laboratory, National Oceanic and Atmospheric Administration, Boulder, CO, USA, [4]School of Earth and Space Sciences, University of Science and Technology of China, Hefei, China

Abstract The Pinatubo eruption in 1991 injected 10–20 Tg SO_2 into the stratosphere, which formed sulfate aerosols through oxidation. Our modeling results show that volcanic heating significantly perturbs the heterogeneous and homogeneous chemistry including NO_x and HO_x catalytic cycles in the tropical stratosphere. The simulated tropical chemical ozone tendency is positive at 20 mb while negative at 10 mb in the tropics. The simulated ozone chemical tendency is of the same magnitude as the dynamical ozone tendency caused by the accelerated tropical upwelling, but with the opposite sign. Our study finds that the tropical ozone chemical tendency due to homogeneous chemistry becomes more important than heterogeneous chemistry 3 months after eruption. Sensitivity simulations further suggest that the tropical ozone tendency through heterogeneous chemistry is saturated when the injected amount exceeds 2 Tg.

Plain Language Summary In 1991, a large volcanic eruption injected 10–20 Tg SO_2 into the stratosphere and perturbed the stratospheric chemistry and dynamics. In this study, we use a climate model to quantify the chemical and dynamical influence of the volcano on tropical stratospheric ozone. Model suggests that the ozone chemical tendency is positive around 28 km while negative around 35 km. Our study also suggests that both heterogeneous and homogeneous chemical reactions contribute to the ozone anomalies. With sensitivity studies, we show that the tropical ozone changes due to heterogeneous chemistry is saturated if the injected amount exceeds 2 Tg.

1. Introduction

The eruption of Mt. Pinatubo in 1991 increased the global stratospheric aerosol loading by one order of magnitude for about 2 years. Satellite and in situ observations showed that the 1991 Pinatubo eruption depleted the tropical total column ozone (TCO) by 6%–8% (McCormick et al., 1995; Schoeberl et al., 1993), with a 20% local reduction 24–25 km above the Brazzaville site located at 4°S, 15°E (Grant et al., 1992). A TCO depletion of about 10%–15% was observed when the Pinatubo aerosols were transported to the Antarctic stratosphere in late September 1991, which was mainly a result of accelerated heterogeneous chemistry on the surface of Pinatubo sulfate aerosols and polar stratospheric clouds (Brasseur & Granier, 1992; Hofmann et al., 1992; Portmann et al., 1996; Solomon et al., 1993).

Tropical stratospheric ozone production and loss is governed by the Chapman cycle and the catalytic cycles involving active halogens (ClO_x, BrO_x), nitrogen (NO_x) and hydrogen (HO_x) (McCormick et al., 1995; Solomon, 1999). On the one hand, the enhanced aerosol surface area density (SAD) due to 1991 Pinatubo eruption provided reaction surfaces for hydrolysis of dinitrogen pentoxide (N_2O_5), which depletes NO_x and suppresses ozone depletion via the NO_x catalytic cycle (Aquila et al., 2013; Fahey et al., 1993; Solomon et al., 1996). On the other hand, reduction of NO_x increases concentrations of ClO_x and HO_x, which promotes ozone depletion via the odd hydrogen catalytic cycles in the lower stratosphere (Granier & Brasseur, 1992; Hofmann & Solomon, 1989; Solomon et al., 1993; Tabazadeh et al., 2002; Tie & Brasseur, 1995).

The long-term radiative effect is mostly controlled by sulfate aerosol (Labitzke & McCormick, 1992; Stenchikov et al., 2021), while the short-term radiative effect is heavily influenced by the volcanic ash and SO_2 during the first weeks (Osipov et al., 2020; Stenchikov et al., 2021; Zhu et al., 2020). Because our study focuses on the long-term radiative effect, the short-term heating by the volcanic ash and SO_2 is not considered. Consequently, the tropical upwelling was accelerated (Aquila et al., 2012; Kinne et al., 1992; Pitari & Mancini, 2002) and the

latitudinal distributions of ozone and other chemical tracers were perturbed (Lin & Fu, 2013; Revell et al., 2012). In addition to the dynamical feedback, the reaction rates of catalytic cycles changed in response to stratospheric warming (Lippmann et al., 1980; Michael et al., 1981; Mozurkewich & Calvert, 1988; Van Doren et al., 1990). Previous studies have focused primarily on heterogeneous and radiative-dynamical effects (Aquila et al., 2013; Kilian et al., 2020; Muthers et al., 2015; Telford et al., 2009). The radiative-catalytic effect and its relative contribution to the tropical net ozone production anomalies have not been explicitly quantified.

Heterogeneous chemistry like the hydrolysis of N_2O_5 on liquid sulfate aerosols is saturated when the aerosol SAD anomaly is above a certain threshold, which varies by region (Fahey et al., 1993; Prather, 1992). However, the radiative-catalytic effect is not limited by aerosol SAD directly. Therefore, the relative contributions of the heterogeneous reactions and radiative-catalytic cycles to the net ozone production anomalies depend on the injection amount. It is necessary to separate the radiative-catalytic effect from heterogeneous chemistry and radiative-dynamical effects to predict the ozone change resulting from volcanic or stratospheric aerosol injection (solar radiation management) scenarios with various injection amounts and locations.

In this study, we use the Community Earth System Model-Whole Atmosphere Community Climate Model (CESM-WACCM) to simulate the chemical and dynamical impacts on the ozone production rate due to the 1991 Pinatubo eruption. Satellites and in situ measurements of stratospheric aerosols and gaseous tracers (ozone and SO_2) are compared against the model. With the model validated, we attribute the modeled tropical ozone net production anomalies to the heterogeneous reaction effect (denoted by S'_{het}), the radiative-catalytic effect (denoted by S'_{hom}) and the radiative-dynamical effect (i.e., acceleration of the Brewer-Dobson circulation (BDC), denoted by B'). Finally, sensitivity simulations are performed to evaluate the relative contribution of the heterogeneous reactions and radiative-catalytic cycles to the ozone production rate.

2. Methods

2.1. Model Experiments

We use the Community Earth System Model-Whole Atmosphere Community Climate Model, version 1 (CESM1-WACCM) (Hurrell et al., 2013) coupled with the three-mode version of the Modal Aerosol Model (Liu et al., 2012) to study the stratospheric ozone response to the Pinatubo eruption. Based on SO_2 observations from the Total Ozone Mapping Spectrometer (TOMS) and the Television Infrared Observation Satellite (TIROS) satellites, we inject 12 Tg SO_2 into the nearest grid cells between 12:00 and 18:00 UTC on 15 June 1991 in the "full" simulation scenario (Table S1 in Supporting Information S1) (Guo, Bluth, et al., 2004; Guo, Rose, et al., 2004; Mills et al., 2016). In this study, the injections of volcanic ash, halogen species and water vapor emission are not considered. We run the model from 1 January 1990 to 31 December 1995 with a 5-year model spin-up. The simulated three-dimensional wind is nudged (i.e., UV nudging, Davis et al., 2020; Schmidt et al., 2018) toward the Modern-Era Retrospective analysis for Research and Applications, Version 2 (MERRA-2) reanalysis (Gelaro et al., 2017). Shown in Figure S1 of the Supporting Information S1, the simulated magnitude and spatial distribution of the tropical residual velocity (w^*) by CESM1-WACCM is similar to that calculated from MERRA-2. We also note that the nudged experiments don't resolve the full radiative and dynamical feedbacks from Pinatubo. The nudged simulations with (the "full" scenario) and without (the "novolc" scenario) Pinatubo are performed to calculate the anomalies of aerosols and ozone due to the Pinatubo eruption. Simulations with the radiation and heterogeneous chemistry turned off ("norad" and "nohet" scenarios, respectively) are performed to diagnose the relative contributions due to volcanic heating and increased aerosol SAD. Details of the model configurations are provided in Texts S1 and S2 in Supporting Information S1.

2.2. Residual Velocity and the TEM Continuity Equation

The BDC transports ozone poleward (Brewer, 1949; Dobson, 1956). In order to diagnose the zonal-mean change in stratospheric ozone due to Pinatubo, we use the Transformed Eulerian-Mean (TEM) formulation of the zonal-mean ozone continuity equation with spherical coordinates. Details of TEM continuity equation are provided in Text S3 of the Supporting Information S1.

According to the TEM continuity equation (Equation S9 in Supporting Information S1), the ozone anomalies due to Pinatubo relative to the climatology can be divided into three terms: (a) the BDC transport anomaly (denoted by

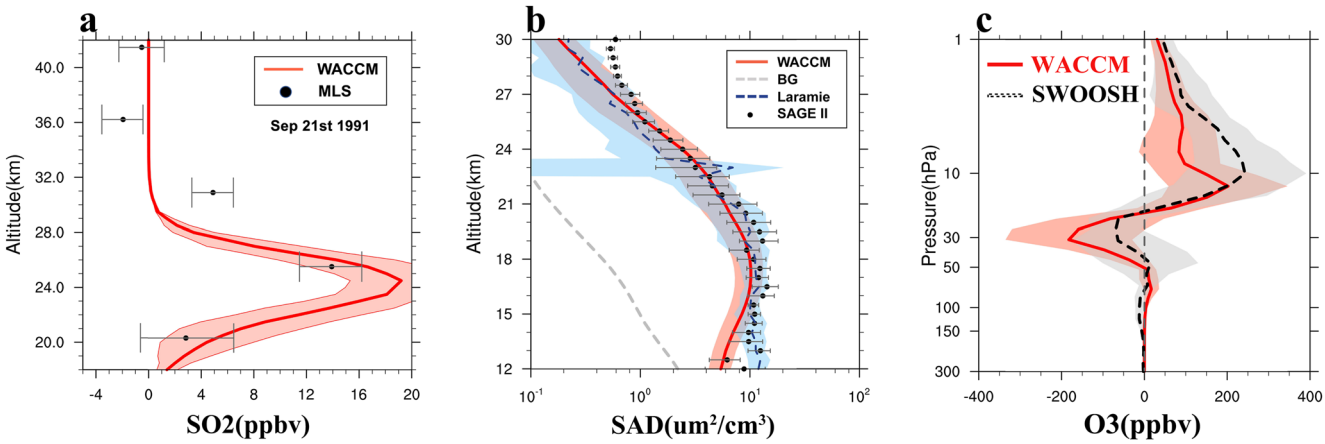

Figure 1. Comparison between the observed and simulated SO_2 (ppbv), surface area density (SAD) ($\mu m^2/cm^3$), NO_2 percentage anomaly (%), and O_3 (ppbv). (a) The simulated vertical distribution of the zonal averaged SO_2 between 10°S and the equator on 21 September 1991 is shown by the red line. The red shading denotes the modeled variability (one standard deviation, σ). The observations from Microwave Limb Sound are denoted by the black dots with error bars according to Read et al. (1993). (b) The vertical distribution of SAD observed by the balloon-borne optical particle counter at Laramie (41°N, 105°W) averaged from June 1991 to May 1993 is shown by the blue dashed line. Observations by SAGE II near Laramie averaged between June 1991 and May 1993 are denoted by the black dots with error bars. Simulated SAD near Laramie averaged between June 1991 and May 1993 is denoted by the red line. Simulated SAD in the non-volcanic conditions is shown by the gray dashed line. Error bars and shading in this panel denote 0.5σ. (c) The red line denotes the simulated ozone anomaly averaged between 30°S and 30°N from June 1991 to May 1993 relative to the simulated mean ozone concentrations between 1990 and 1995. The black dashed line shows the ozone anomaly in Stratospheric Water and Ozone Satellite Homogenized. The shading in this panel denotes 0.5σ of this period.

B'), (b) the eddy transport anomaly (E') and (c) the chemical term anomaly (S'_{chem}). In this study, we focus mainly on the anomalies of the chemical term (S'_{chem}). We further separate S'_{chem} into two processes: (a) the heterogeneous chemical term due to increased SAD (S'_{het}) and (b) the gas-phase chemical term in response to radiative-catalytic effect (S'_{hom}). Note that ozone radiative feedback is included in both S'_{het} and S'_{hom} terms. The perturbation in photochemical rates due to actinic flux reduction is included in term S'_{hom}. Note that the non-linearity relationship does exist between S'_{hom} and S'_{het}, but it's less than 1% above 30 mb in the tropics (Figure S2 in Supporting Information S1). In this study, we focus on the tropical stratosphere above 30 mb, where the eddy ozone transport term is smaller than BDC and chemical terms in tropics above 30 mb (Miyazaki et al., 2005). The anomalies of the chemical and BDC terms are diagnosed by various simulation scenarios shown in Equations 1–4.

$$B' = B_{full} - B_{novolc} \quad (1)$$

$$S'_{chem} = S_{full} - S_{novolc} \quad (2)$$

$$S'_{hom} = S_{full} - S_{norad} - (S_{novolc} - S_{BG\_norad}) \quad (3)$$

$$S'_{het} = S_{full} - S_{nohet} - (S_{novolc} - S_{BG\_nohet}) \quad (4)$$

3. Results

As shown in Figure 1, the simulated vertical profiles of SO_2, aerosol SAD, and ozone are compared with satellite observations. Figure 1a shows that the altitudes of the maximum SO_2 concentrations between 10°S and the equator on 21 September 1991 were around 24–25 km, which agrees with the Microwave Limb Sound observations. Figure 1b shows that the stratospheric aerosol SAD was elevated by one order of magnitude in both observations and simulations. Satellite observations by Stratospheric Aerosol and Gas Experiment II (SAGE II) and balloon-borne optical particle counters at Laramie (41°N, 105°W, Kovilakam & Deshler, 2015) show that the aerosol SAD averaged from June 1991 to May 1993 was about 10 $\mu m^2/cm^3$ between 12 and 20 km. The observed SAD decreased by over one order of magnitude from 20 to 30 km. Modeled stratospheric SAD was within the observed variability (0.5 times standard deviation) above 15 km. The model underestimated the observed SAD below 15 km by ~20%. Compared with the simulation without Pinatubo, the stratospheric SAD near Laramie

averaged from June 1991 to May 1993 was elevated by 1–2 orders of magnitude. As shown in Figure S3 of the Supporting Information S1, the poleward transport of Pinatubo aerosol optical depth in the mid-visible range was observed by the AVHRR) satellite and simulated by the model.

Consistent with the Stratospheric Water and Ozone Satellite Homogenized (SWOOSH) data set (Davis et al., 2016), the simulated ozone anomalies averaged between 30°S and 30°N and from June 1991 to May 1993 exhibit a dipole distribution with positive ozone anomalies near 10 mb and negative anomalies near 30 mb (Figure 1c). Similar dipole distribution of ozone anomalies after 1991 Pinatubo eruption were observed by electrochemical concentration cell ozonesondes at Brazzaville, Congo (4°S, 15°E) (Grant et al., 1992); Boulder, Colorado (40°N) and Wallops Island, Virginia (38°N) (Hofmann et al., 1994). The observed tropical TCO and its temporal and spatial variabilities can be reproduced in our simulation (Figure S4 in Supporting Information S1). Shown in Figure S5 of the Supporting Information S1, similar TCO anomalies was also simulated by Telford et al. (2009). A temperature dipole distribution is also simulated by WACCM and captured in the MERRA-2 reanalysis data set (Figure S6 in Supporting Information S1). In addition, the NO_x was depleted significantly via the hydrolysis of N_2O_5 on the increased aerosol SAD (Aquila et al., 2013; Fahey et al., 1993; Solomon et al., 1996). Shown in Figure S7 of the Supporting Information S1, the simulated percentage anomalies of stratospheric NO_2 column density are within the observed variability (one standard deviation) of UV/Vis spectrophotometer observation at Lauder (Johnston & McKenzie, 1984) with the maximum depletion of about 40%–50% from October 1991 to June 1992. In summary, the simulation scenario "full" with 12 Tg SO_2 injection can capture the characteristics of aerosols, O_3, NO_2, and SO_2 after Pinatubo eruption.

As shown in Figure 2, the simulated largest change in the ozone production rate (anomalies of chemical tendency S'_{chem} in the mixing ratio, with a unit of ppbv per second) due to Pinatubo aerosols occurred in the tropical stratosphere. A dipole of S'_{chem} is simulated, with positive S'_{chem} in the TB box (30–12.5 mb, 30°S–30°N) and negative S'_{chem} in the TU box (11–3.5 mb, 30°S–30°N). The positive ozone tendency in TB box is mainly due to NO_x depletion, while the negative tendency in TU box is mostly resulted from HO_x increase, respectively (Tilmes et al., 2018). The simulated anomaly in the midlatitude and polar regions are more visually obvious (Figure S8 in Supporting Information S1) when the rate anomaly expressed in concentration units (i.e., molecules/cm^3/s). Consistent with previous studies (Tilmes et al., 2018), negative anomalies of ozone production rates are simulated in the Antarctic lower stratosphere, attributed mainly to heterogeneous chemistry, which releases reactive halogen species (Fahey et al., 1993; Solomon, 1999; Tilmes et al., 2008). In the tropical stratosphere (the TU and TB boxes in Figure 2), the ozone net production rate is dominated by catalytic cycles, including the reactive nitrogen cycle (NO_x-cycle) in the TB box (Meul et al., 2014; Tilmes et al., 2009, 2018), while SO_2/SO_4 effects are more important when the injection amount well exceeds that of Pinatubo (Osipov et al., 2021). An ozone chemical net production rate anomaly dipole is simulated, with a positive anomaly (i.e., net production) in the TB box and negative anomalies (i.e., net chemical loss) in the TU box (Figure 2a). We decompose the simulated chemical anomaly into two terms, one from the change in the catalytic cycle rate through radiative feedback (S'_{hom}), shown in Figure 2c, and one from the change through heterogeneous reactions (S'_{het}), shown in Figure 2d. Both of these terms display a dipole distribution with the same phase, similar to the total chemical term (S'_{chem}). The simulated S'_{hom} is overall larger by a factor of 440% than S'_{het} and dominates the chemical production anomaly of ozone in the tropical stratosphere.

The warmed stratosphere due to Pinatubo volcanic heating can change the transport of chemical tracers (Lin & Fu, 2013; Revell et al., 2012) as well as the catalytic cycle reaction rates, which are temperature dependent (Lippmann et al., 1980; Michael et al., 1981). The NO_x production rate slows down in the TB box through $N_2O + O^1D$ as a result of the combined effect of a smaller rate constant ($K_{N2O+O1D}$) in warmer conditions and decreased NO_y due to accelerated BDC. The negative tendency of NO_x slows the ozone loss reaction via the NO_x catalytic cycle with the simulated positive S'_{hom}. In addition, volcanic heating slows the ozone production rate by decreasing K_{O+O2} in warmer conditions. The anomaly of the chemical tendency via gas-phase chemistry (S'_{hom}) is negative in the TU zone due to the faster HO_x catalytic ozone loss cycle and the resultant slower ozone production rate.

For the S'_{het} term, the loss of NO_x through the hydrolysis of N_2O_5 suppresses the catalytic NO_x ozone loss cycle, and consequently there is a positive ozone net chemical production rate in the TB box. In the TU box, the active hydrogen cycle (HO_x-cycle) and active chlorine and bromine cycle ($ClO_x + BrO_x$) dominate (Lary, 1997; Tilmes et al., 2018). NO_x is a sink for active hydrogen (HO_x) and chlorine (ClO_x) (Fahey et al., 1993; Rodriguez et al., 1994; Tie & Brasseur, 1995), and the loss of NO_x via the heterogeneous reaction increases HO_x and ClO_x

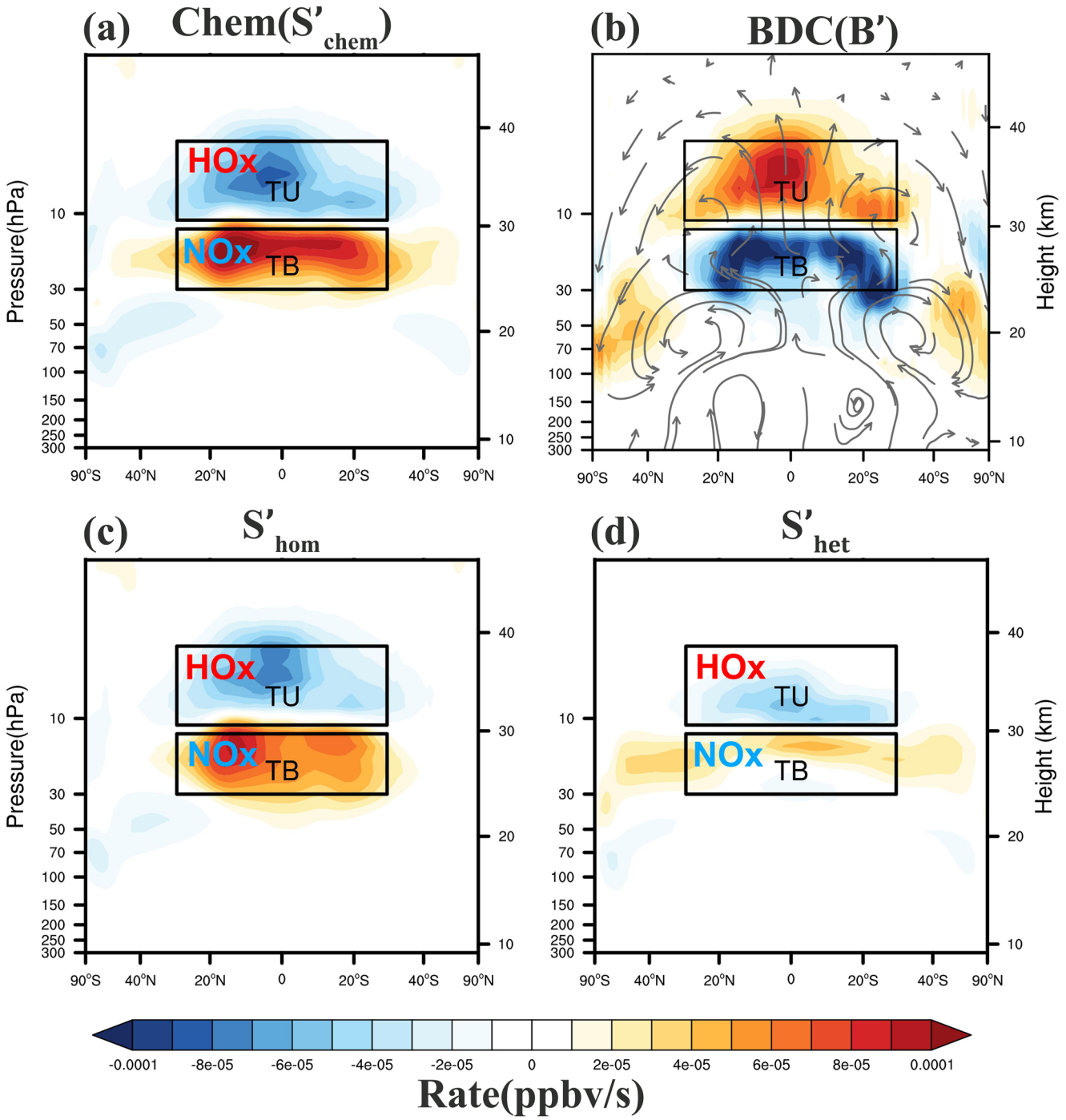

Figure 2. The simulated ozone tendency (ppbv/s) anomaly averaged from June 1991 to May 1993 due to various terms including gas-phase chemistry (S'_{hom}), heterogeneous chemistry (S'_{het}), and Brewer-Dobson circulation (BDC) transport (B'). (a) The latitudinal (cosine weighted) and vertical distribution of the chemical process and the change in the ozone production rate (simulation scenario "full" minus "novolc"). (b) Same as (a) but for the BDC effect diagnosed by the Transformed Eulerian-Mean continuity equation (simulation scenario "full" minus "novolc"); the residual circulation anomalies are denoted by the streamlines. (c) Same as (a) but for the gas-phase chemistry (simulation scenario difference between "full" and "norad" minus the difference between "novolc" and "BG_norad"). (d) Same as (a) but for the heterogeneous chemistry (simulation scenario difference between "full" and "nohet" minus the difference between "novolc" and "BG_nohet"). Simulations for calculations in all panels are from the scenarios with and without 12 Tg SO_2 injected. The black rectangular boxes denote the zones of interest in this study. The tropical bottom box (TB) covers the region of 30–12.5 hPa, 30°S–30°N; the tropical upper box (TU) covers the region of 11–3.5 hPa, 30°S–30°N.

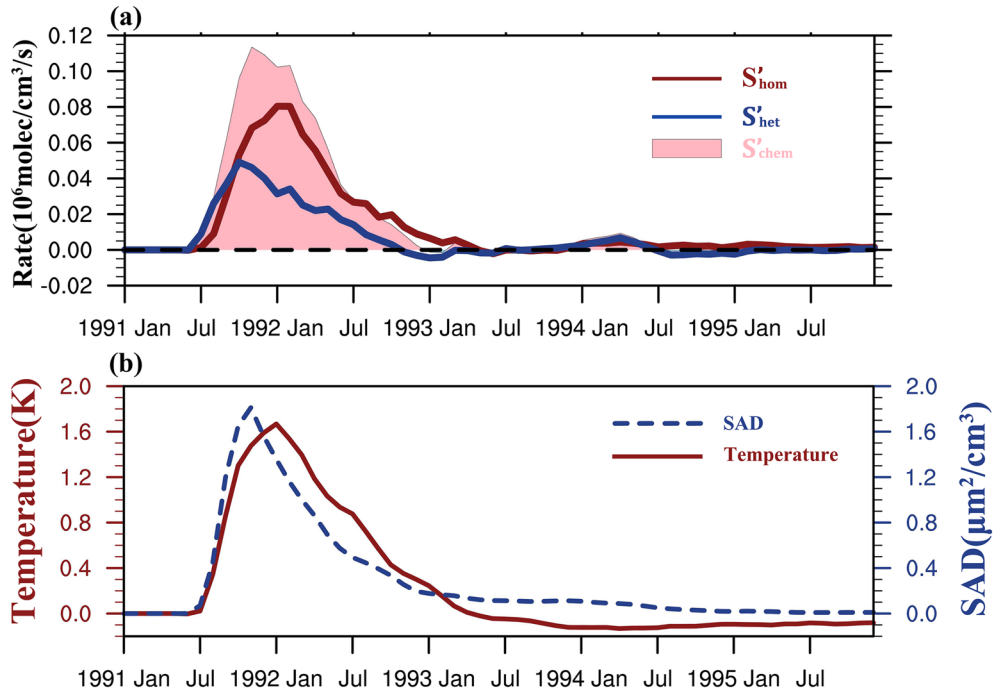

Figure 3. (a) Simulated monthly ozone production rate anomalies (molec/cm^3/s) at 15 hPa over 30°S–30°N due to the gas-phase chemistry (simulation scenario difference between "full" and "norad" minus the difference between "novolc" and "BG_norad") is shown by the red line; The anomaly due to the heterogeneous chemistry (simulation scenario difference between "full" and "nohet" minus the difference between "novolc" and "BG_nohet") is denoted by the blue line; The anomaly due to the total chemical effect (simulation scenario "full" minus "novolc") is denoted by the shadow; (b) Simulated temperature anomalies (K) at 15 hPa (simulation scenario "nohet" minus "BG_nohet") are denoted by red solid line; the aerosol surface area density anomalies ($\mu m^2 \cdot cm^{-3}$) at 15 hPa (simulation scenario "norad" minus "BG_norad") are denoted by the blue dash line. Simulations for calculation in all panels are from the scenarios with and without 12 Tg SO_2 injected.

ozone loss cycles. Similar ozone anomalies were found using simulations with and without Pinatubo SAD (Kilian et al., 2020; Muthers et al., 2015).

In Equation S9 in Supporting Information S1, the net ozone tendency is governed by the chemical term (S), the BDC transport term (B), and the eddy transport term (E). BDC transports tropical ozone to higher altitudes and latitudes (Brewer, 1949; Dobson, 1956). As shown in Figure S6 of the Supporting Information S1, the stratosphere is heated globally, with a tropical lower stratosphere temperature anomaly of about 2 K averaged from June 1991 to May 1993. Similar to Aquila et al. (2013), Figure 2b shows that the simulated BDC is accelerated in response to volcanic heating. Anomalies of residual circulation are denoted by the streamlines showing the tropical particles upwelling and then moving poleward. The climatological ozone shows that the TB box is sort of ozone peak, and is greater compared with the TU box. The accelerated BDC transports richer ozone upward in the tropical stratosphere, with a negative ozone tendency in the TB box and a positive ozone tendency in the TU box. The simulated BDC-induced ozone tendency anomaly is of the same magnitude as the simulated chemical tendency shown in Figure 2a, but with the opposite phase.

Figure 3a compares the temporal distributions between S'_{hom} and S'_{het} in the TB box at 15 mb from January 1991 to December 1995. Consistent with the simulated temperature anomaly shown in Figure 3b, S'_{hom} reaches a maximum in late 1991 and early 1992 and decays to negligible levels 2 years after the Pinatubo eruption. The chemical tendency due to heterogeneous chemistry (S'_{het}) grows rapidly in the first few months after Pinatubo erupts and decays to a negligible level by July 1993, when the volcanic sulfate aerosol SAD decays below 0.1 $\mu m^2/cm^3$, as shown in Figure 3b. Shown in Figure 3a, about two thirds of the chemical change in ozone concentration at 15 mb (tendency integrated over time) is attributed by the change in gas-phase chemistry (S'_{hom}); while the remaining one third is attributed by the change in the heterogeneous chemistry (S'_{het}).

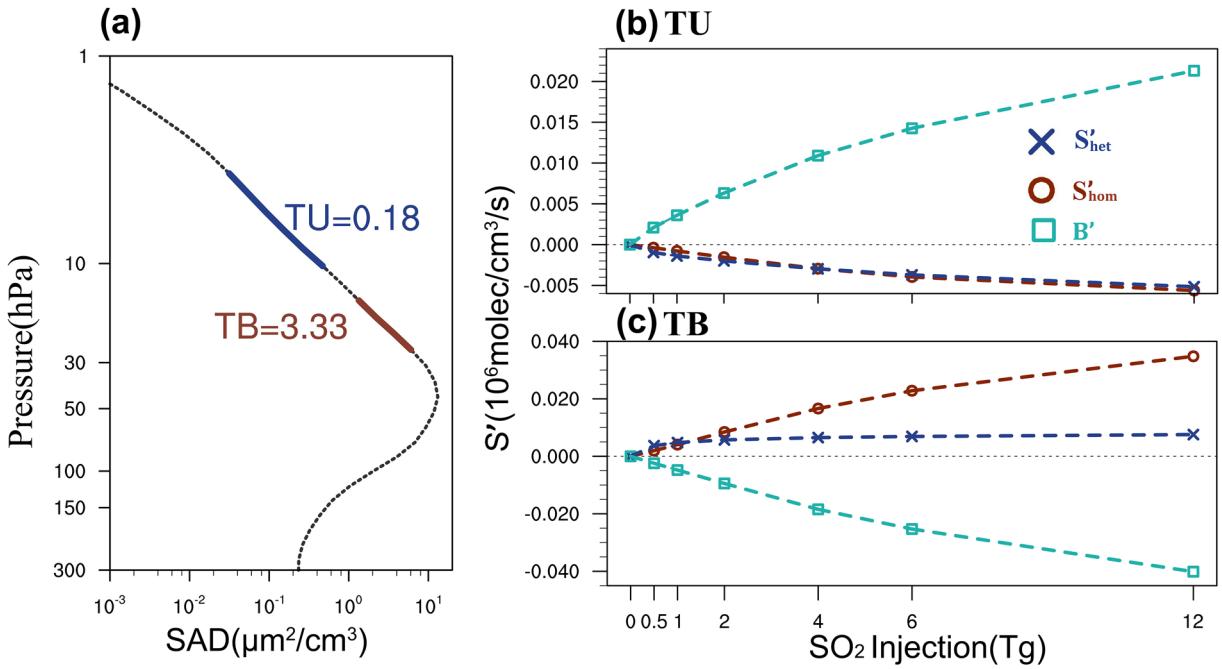

Figure 4. (a) The vertical distribution of surface area density (SAD) averaged from June 1991 to May 1993 over 30°S–30°N. The thick blue line and text denote the aerosol SAD in TU zone; the thick red line and text denote the aerosol SAD in TB zone. (b) The sensitivity of ozone production rate (molec/cm^3/s) over TB box averaged from June 1991 to May 1993 to the amount of SO_2 injected. The red circle denotes the change of ozone production rate due to gas-phase chemistry (simulation scenario difference between "full" and "norad" minus the difference between "novolc" and "BG_norad") with equivalent mass of SO_2 injected; the change of heterogeneous chemistry (simulation scenario difference between "full" and "nohet" minus the difference between "novolc" and "BG_nohet") is shown by the blue cross; the ozone tendencies due to Brewer-Dobson circulation is shown by green squares. (c) Same as (b) but over TU box.

4. Sensitivity Tests

Sensitivity simulations are conducted with various injected amounts of SO_2 (i.e., 6.0, 4.0, 2.0, 1.0, and 0.5 Tg) to diagnose the dependence of S'_{hom} and S'_{het} on the simulated volcanic aerosols. As shown in Figure 4a, 98% of the 2-year averaged tropical SAD anomaly is located below 15 mb. In the TB box, the increasing rate of S'_{het} with the injection amount decreases quickly with injected amounts above 1 Tg (Figure 4b). The saturation of S'_{het} is because under high load of aerosol, N_2O_5 is converted to HNO_3 as fast as it can be formed. The net conversion rate of NO_x to HNO_3 becomes independent of the aerosol loading (Fahey et al., 1993; Prather, 1992; Rodriguez et al., 1991; Solomon, 1999). A similar saturation threshold was reported by Berthet et al. (2017), in which changes to NO_x and HNO_3 induced by the Sarychev eruption (0.9 Tg) were comparable to those of Pinatubo due to saturation. In contrast, S'_{hom} increase near linearly with injection amount. Our study suggests that in the TB box, both terms contribute to the net ozone chemical production rate anomaly nearly equally when the amount of injected SO_2 is less than 2 Tg. S'_{hom} becomes increasingly dominant when the injected amount exceeds 2 Tg. The negative anomaly of the ozone tendency due to accelerated BDC (B') increases with injection amount and offsets the positive ozone tendency anomaly due to S'_{hom}. Shown in Figure 4b, in the TU box, where the HO_x cycle dominates, limited aerosol SAD anomalies are modeled (not saturated) compared with TB box in the Pinatubo scenario (Figure 4a). Both S'_{het} and S'_{hom} are negative and contribute nearly equally to the net ozone chemical production rate with various injection scenarios. The transport impact from the accelerated BDC (B') dominates the ozone tendency in TU box.

5. Conclusions

The Pinatubo eruption in 1991 injected 10–20 Tg SO_2 into the stratosphere and perturbed the stratospheric chemistry. The WACCM-MAM3 is used to study the contributions from gas-phase and heterogeneous chemistry to the anomalies of the stratospheric ozone tendency. Simulated anomalies of aerosols, SO_2, NO_2, and ozone following the Pinatubo eruption are compared and validated against satellite and balloon-borne in situ measurements.

Model simulations with volcanic heating and heterogeneous chemistry turned on and off suggest that the largest ozone production rate anomalies occurred in the tropical stratosphere, with positive ozone production centered at ∼10 mb, and negative ozone production centered at ∼20 mb. The simulated dipole in the ozone production rate anomaly in the tropics is due to changes in both gas-phase chemistry (e.g., NO_x and HO_x catalysis cycles) and heterogeneous chemistry (e.g., N_2O_5 hydrolysis). Previous studies show that heating from volcanic sulfate aerosols causes tropical upwelling and extratropical downwelling (Aquila et al., 2012, 2013). The accelerated tropical upwelling redistributes the stratospheric ozone, with a positive tendency at ∼10 mb and a negative tendency at ∼20 mb. The simulated chemical tendency of the ozone is of the same magnitude as the dynamical tendency, but opposite in sign. In the tropics, the ozone change due to enhanced BDC is dominant, and it can offset the chemical tendencies, showing ozone net loss in the TB box and ozone net gain in the TU box.

Our study finds that 3–5 months after the Pinatubo eruption, the tropical ozone chemical tendency due to volcanic heating is more important than that caused by heterogeneous reactions on the surfaces of sulfate. Sensitivity studies further suggest that the ozone tendency due to heterogeneous chemistry is saturated when the injected mass is greater than 2 Tg, while the ozone tendency due to the gas-phase chemistry as well as the BDC transport is not limited by saturation effect.

Data Availability Statement

The publicly available data can be downloaded via the following URLs: The SWOOSH data can be downloaded via https://csl.noaa.gov/groups/csl8/swoosh/; SAGE II can be downloaded via https://figshare.com/s/c48bba68f5eafbbd7903; the NDACC Measurements at the station in Lauder, New Zealand, can be downloaded via https://figshare.com/s/c48bba68f5eafbbd7903; the MERRA-2 forcing data can be downloaded via https://rda.ucar.edu/datasets/ds313.3/; the in situ aerosol measurements at Laramie can be downloaded via http://www-das.uwyo.edu/~deshler/Data/Aer_Meas_Wy_read_me.htm; the AVHRR satellite data can be downloaded via https://www.ncei.noaa.gov/products/climate-data-records/avhrr-aerosol-optical-thickness. Model simulations can be downloaded via https://figshare.com/s/c48bba68f5eafbbd7903.

Acknowledgments
This work is supported by the National Natural Science Foundation of China (42121004, 42130601, 42175089). The CESM-WACCM project is supported by the National Science Foundation and the Office of Science (BER) of the U.S. Department of Energy. The authors are grateful to the High-Performance Computing Public Service Platform of Jinan University and Lanzhou University.

References

Aquila, V., Oman, L. D., Stolarski, R., Douglass, A. R., & Newman, P. A. (2013). The response of ozone and nitrogen dioxide to the eruption of Mt. Pinatubo at southern and northern midlatitudes. *Journal of the Atmospheric Sciences*, *70*(3), 894–900. https://doi.org/10.1175/JAS-D-12-0143.1

Aquila, V., Oman, L. D., Stolarski, R. S., Colarco, P. R., & Newman, P. A. (2012). Dispersion of the volcanic sulfate cloud from a Mount Pinatubo–like eruption. *Journal of Geophysical Research*, *117*(D6), D06216. https://doi.org/10.1029/2011JD016968

Berthet, G., Jégou, F., Catoire, V., Krysztofiak, G., Renard, J. B., Bourassa, A. E., et al. (2017). Impact of a moderate volcanic eruption on chemistry in the lower stratosphere: Balloon-borne observations and model calculations. *Atmospheric Chemistry and Physics*, *17*(3), 2229–2253. https://doi.org/10.5194/acp-17-2229-2017

Brasseur, G., & Granier, C. (1992). Mount Pinatubo aerosols, chlorofluorocarbons, and ozone depletion. *Science*, *257*(5074), 1239–1242. https://doi.org/10.1126/science.257.5074.1239

Brewer, A. W. (1949). Evidence for a world circulation provided by the measurements of helium and water vapor distribution in the stratosphere. *Quarterly Journal of the Royal Meteorological Society*, *75*(326), 351–363. https://doi.org/10.1002/qj.49707532603

Davis, N. A., Davis, S. M., Portmann, R. W., Ray, E., Rosenlof, K. H., & Yu, P. (2020). A comprehensive assessment of tropical stratospheric upwelling in the specified dynamics community Earth system model 1.2.2—Whole atmosphere community climate model (CESM (WACCM)). *Geoscientific Model Development*, *13*(2), 717–734. https://doi.org/10.5194/gmd-13-717-2020

Davis, S. M., Rosenlof, K. H., Hassler, B., Hurst, D. F., Read, W. G., Vömel, H., et al. (2016). The stratospheric water and ozone satellite homogenized (SWOOSH) database: A long-term database for climate studies. *Earth System Science Data*, *8*(2), 461–490. https://doi.org/10.5194/essd-8-461-2016

Dobson, G. M. B. (1956). Origin and distribution of polyatomic molecules in the atmosphere. *Proceedings of the Royal Society A: Mathematical, Physical and Engineering Sciences*, *A236*, 187–193. https://doi.org/10.1098/rspa.1956.0127

Fahey, D. W., Kawa, S. R., Woodbridge, E. L., Tin, P., Wilson, J. C., Jonsson, H. H., et al. (1993). In situ measurements constraining the role of sulphate aerosols in mid-latitude ozone depletion. *Nature*, *363*(6429), 509–514. https://doi.org/10.1038/363509a0

Gelaro, R., McCarty, W., Suárez, M. J., Todling, R., Molod, A., Takacs, L., et al. (2017). The modern-era retrospective analysis for research and applications, version 2 (MERRA-2). *Journal of Climate*, *30*(14), 5419–5454. https://doi.org/10.1175/JCLI-D-16-0758.1

Granier, C., & Brasseur, G. (1992). Impact of heterogeneous chemistry on model predictions of ozone changes. *Journal of Geophysical Research*, *97*(D16), 18015–18033. https://doi.org/10.1029/92JD02021

Grant, W. B., Fishman, J., Browell, E. V., Brackett, V. G., Nganga, D., Minga, A., et al. (1992). Observations of reduced ozone concentrations in the tropical stratosphere after the eruption of Mt. Pinatubo. *Geophysical Research Letters*, *19*(11), 1109–1112. https://doi.org/10.1029/92GL01153

Guo, S., Bluth, G. J. S., Rose, W. I., Watson, I. M., & Prata, A. J. (2004). Re-evaluation of SO_2 release of the 15 June 1991 Pinatubo eruption using ultraviolet and infrared satellite sensors. *Geochemistry, Geophysics, Geosystems*, *5*(4), Q04001. https://doi.org/10.1029/2003GC000654

Guo, S., Rose, W. I., Bluth, G. J. S., & Watson, I. M. (2004). Particles in the great Pinatubo volcanic cloud of June 1991: The role of ice. *Geochemistry, Geophysics, Geosystems*, *5*(5), Q05003. https://doi.org/10.1029/2003GC000655

Hofmann, D. J., Oltmans, S. J., Harris, J. M., Solomon, S., Deshler, T., & Johnson, B. J. (1992). Observation and possible causes of new ozone depletion in Antarctica in 1991. *Nature*, *359*(6393), 283–287. https://doi.org/10.1038/359283a0

Hofmann, D. J., Oltmans, S. J., Komhyr, W. D., Harris, J. M., Lathrop, J. A., Langford, A. O., et al. (1994). Ozone loss in the lower stratosphere over the United States in 1992–1993: Evidence for heterogeneous chemistry on the Pinatubo aerosol. *Geophysical Research Letters*, *21*(1), 65–68. https://doi.org/10.1029/93GL02526

Hofmann, D. J., & Solomon, S. (1989). Ozone destruction through heterogeneous chemistry following the eruption of El Chichón. *Journal of Geophysical Research*, *94*(D4), 5029–5041. https://doi.org/10.1029/JD094iD04p05029

Hurrell, J. W., Holland, M. M., Gent, P. R., Ghan, S., Kay, J. E., Kushner, P. J., et al. (2013). The community Earth system model: A framework for collaborative research. *Bulletin of the American Meteorological Society*, *94*(9), 1339–1360. https://doi.org/10.1175/BAMS-D-12-00121.1

Johnston, P. V., & McKenzie, R. L. (1984). Long-path absorption measurements of tropospheric NO_2 in rural New Zealand. *Geophysical Research Letters*, *11*(1), 69–72. https://doi.org/10.1029/GL011i001p00069

Kilian, M., Brinkop, S., & Jöckel, P. (2020). Impact of the eruption of Mt Pinatubo on the chemical composition of the stratosphere. *Atmospheric Chemistry and Physics*, *20*(20), 11697–11715. https://doi.org/10.5194/acp-20-11697-2020

Kinne, S., Toon, O. B., & Prather, M. J. (1992). Buffering of stratospheric circulation by changing amounts of tropical ozone a Pinatubo case study. *Geophysical Research Letters*, *19*(19), 1927–1930. https://doi.org/10.1029/92GL01937

Kovilakam, M., & Deshler, T. (2015). On the accuracy of stratospheric aerosol extinction derived from in situ size distribution measurements and surface area density derived from remote SAGE II and HALOE extinction measurements. *Journal of Geophysical Research: Atmospheres*, *120*(16), 8426–8447. Portico. https://doi.org/10.1002/2015jd023303

Labitzke, K., & McCormick, M. P. (1992). Stratospheric temperature increases due to Pinatubo aerosols. *Geophysical Research Letters*, *19*(2), 207–210. https://doi.org/10.1029/91GL02940

Lary, D. J. (1997). Catalytic destruction of stratospheric ozone. *Journal of Geophysical Research*, *102*(D17), 21515–21526. https://doi.org/10.1029/97JD00912

Lin, P., & Fu, Q. (2013). Changes in various branches of the Brewer–Dobson circulation from an ensemble of chemistry climate models. *Journal of Geophysical Research: Atmospheres*, *118*(1), 73–84. https://doi.org/10.1029/2012JD018813

Lippmann, H. H., Jesser, B., & Schurath, U. (1980). The rate constant of $NO+O3 \rightarrow NO_2+O_2$ in the temperature range of 283–443 K. *International Journal of Chemical Kinetics*, *12*(8), 547–554. https://doi.org/10.1002/kin.550120805

Liu, X., Easter, R. C., Ghan, S. J., Zaveri, R., Rasch, P., Shi, X., et al. (2012). Toward a minimal representation of aerosols in climate models: Description and evaluation in the Community Atmosphere Model CAM5. *Geoscientific Model Development*, *5*(3), 709–739. https://doi.org/10.5194/gmd-5-709-2012

McCormick, M. P., Thomason, L. W., & Trepte, C. R. (1995). Atmospheric effects of the Mt Pinatubo eruption. *Nature*, *373*(6513), 399–404. https://doi.org/10.1038/373399a0

Meul, S., Langematz, U., Oberländer, S., Garny, H., & Jöckel, P. (2014). Chemical contribution to future tropical ozone change in the lower stratosphere. *Atmospheric Chemistry and Physics*, *14*(6), 2959–2971. https://doi.org/10.5194/acp-14-2959-2014

Michael, J. V., Allen, J. E., & Brobst, W. D. (1981). Temperature dependence of the nitric oxide+ozone reaction rate from 195 to 369 K. *The Journal of Physical Chemistry*, *85*(26), 4109–4117. https://doi.org/10.1021/j150626a032

Mills, M. J., Schmidt, A., Easter, R., Solomon, S., Kinnison, D. E., Ghan, S. J., et al. (2016). Global volcanic aerosol properties derived from emissions, 1990–2014, using CESM1(WACCM). *Journal of Geophysical Research: Atmospheres*, *121*(5), 2332–2348. https://doi.org/10.1002/2015JD024290

Miyazaki, K., Iwasaki, T., Shibata, K., & Deushi, M. (2005). Roles of transport in the seasonal variation of the total ozone amount. *Journal of Geophysical Research*, *110*(D18), D18309. https://doi.org/10.1029/2005JD005900

Mozurkewich, M., & Calvert, J. G. (1988). Reaction probability of N_2O_5 on aqueous aerosols. *Journal of Geophysical Research*, *93*(D12), 15889–15896. https://doi.org/10.1029/JD093iD12p15889

Muthers, S., Arfeuille, F., Raible, C. C., & Rozanov, E. (2015). The impacts of volcanic aerosol on stratospheric ozone and the Northern Hemisphere polar vortex: Separating radiative-dynamical changes from direct effects due to enhanced aerosol heterogeneous chemistry. *Atmospheric Chemistry and Physics*, *15*(20), 11461–11476. https://doi.org/10.5194/acp-15-11461-2015

Osipov, S., Stenchikov, G., Tsigaridis, K., LeGrande, A. N., & Bauer, S. E. (2020). The role of the SO radiative effect in sustaining the volcanic winter and soothing the Toba impact on climate. *Journal of Geophysical Research: Atmospheres*, *125*(2), e2019JD031726. https://doi.org/10.1029/2019JD031726

Osipov, S., Stenchikov, G., Tsigaridis, K., LeGrande, A. N., Bauer, S. E., Fnais, M., & Lelieveld, J. (2021). The Toba supervolcano eruption caused severe tropical stratospheric ozone depletion. *Communications Earth & Environment*, *2*(1), 71. https://doi.org/10.1038/s43247-021-00141-7

Pitari, G., & Mancini, E. (2002). Short-term climatic impact of the 1991 volcanic eruption of Mt. Pinatubo and effects on atmospheric tracers. *Natural Hazards and Earth System Sciences*, *2*(1/2), 91–108. https://doi.org/10.5194/nhess-2-91-2002

Portmann, R. W., Solomon, S., Garcia, R. R., Thomason, L. W., Poole, L. R., & McCormick, M. P. (1996). Role of aerosol variations in anthropogenic ozone depletion in the polar regions. *Journal of Geophysical Research*, *101*(D17), 22991–23006. https://doi.org/10.1029/96JD02608

Prather, M. (1992). Catastrophic loss of stratospheric ozone in dense volcanic clouds. *Journal of Geophysical Research*, *97*(D9), 10187–10191. https://doi.org/10.1029/92JD00845

Read, W. G., Froidevaux, L., & Waters, J. W. (1993). Microwave limb sounder measurement of stratospheric SO_2 from the Mt. Pinatubo Volcano. *Geophysical Research Letters*, *20*(12), 1299–1302. https://doi.org/10.1029/93GL00831

Revell, L. E., Bodeker, G. E., Smale, D., Lehmann, R., Huck, P. E., Williamson, B. E., et al. (2012). The effectiveness of N_2O in depleting stratospheric ozone. *Geophysical Research Letters*, *39*(15), L15806. https://doi.org/10.1029/2012GL052143

Rodriguez, J. M., Ko, M. K. W., & Sze, N. D. (1991). Role of heterogeneous conversion of N_2O_5 on sulphate aerosols in global ozone losses. *Nature*, *352*(6331), 134–137. https://doi.org/10.1038/352134a0

Rodriguez, J. M., Ko, M. K. W., Sze, N. D., Heisey, C. W., Yue, G. K., & McCormick, M. P. (1994). Ozone response to enhanced heterogeneous processing after the eruption of Mt. Pinatubo. *Geophysical Research Letters*, *21*(3), 209–212. https://doi.org/10.1029/93gl03537

Schmidt, A., Mills, M. J., Ghan, S., Gregory, J. M., Allan, R. P., Andrews, T., et al. (2018). Volcanic radiative forcing from 1979 to 2015. *Journal of Geophysical Research: Atmospheres*, *123*(22), 12491–12508. https://doi.org/10.1029/2018JD028776

Schoeberl, M. R., Bhartia, P. K., Hilsenrath, E., & Torres, O. (1993). Tropical ozone loss following the eruption of Mt. Pinatubo. *Geophysical Research Letters*, *20*(1), 29–32. https://doi.org/10.1029/92GL02637

Solomon, S. (1999). Stratospheric ozone depletion: A review of concepts and history. *Reviews of Geophysics*, *37*(3), 275–316. https://doi.org/10.1029/1999RG900008

Solomon, S., Portmann, R. W., Garcia, R. R., Thomason, L. W., Poole, L. R., & McCormick, M. P. (1996). The role of aerosol variations in anthropogenic ozone depletion at northern midlatitudes. *Journal of Geophysical Research*, *101*(D3), 6713–6727. https://doi.org/10.1029/95JD03353

Solomon, S., Sanders, R. W., Garcia, R. R., & Keys, J. G. (1993). Increased chlorine dioxide over Antarctica caused by volcanic aerosols from Mount Pinatubo. *Nature*, *363*(6426), 245–248. https://doi.org/10.1038/363245a0

Stenchikov, G., Ukhov, A., Osipov, S., Ahmadov, R., Grell, G., Cady-Pereira, K., et al. (2021). How does a Pinatubo-size volcanic cloud reach the middle stratosphere? *Journal of Geophysical Research: Atmospheres*, *126*(10), e2020JD033829. https://doi.org/10.1029/2020JD033829

Tabazadeh, A., Drdla, K., Schoeberl, M. R., Hamill, P., & Toon, O. B. (2002). Arctic "ozone hole" in a cold volcanic stratosphere. *Proceedings of the National Academy of Sciences of the United States of America*, *99*(5), 2609–2612. https://doi.org/10.1073/pnas.052518199

Telford, P., Braesicke, P., Morgenstern, O., & Pyle, J. (2009). Reassessment of causes of ozone column variability following the eruption of Mount Pinatubo using a nudged CCM. *Atmospheric Chemistry and Physics*, *9*(13), 4251–4260. https://doi.org/10.5194/acp-9-4251-2009

Tie, X., & Brasseur, G. (1995). The response of stratospheric ozone to volcanic eruptions: Sensitivity to atmospheric chlorine loading. *Geophysical Research Letters*, *22*(22), 3035–3038. https://doi.org/10.1029/95GL03057

Tilmes, S., Garcia, R. R., Kinnison, D. E., Gettelman, A., & Rasch, P. J. (2009). Impact of geoengineered aerosols on the troposphere and stratosphere. *Journal of Geophysical Research*, *114*(D12), D12305. https://doi.org/10.1029/2008JD011420

Tilmes, S., Müller, R., & Salawitch, R. (2008). The sensitivity of polar ozone depletion to proposed geoengineering schemes. *Science*, *320*(5880), 1201–1204. https://doi.org/10.1126/science.1153966

Tilmes, S., Richter, J. H., Mills, M. J., Kravitz, B., MacMartin, D. G., Garcia, R. R., et al. (2018). Effects of different stratospheric SO_2 injection altitudes on stratospheric chemistry and dynamics. *Journal of Geophysical Research: Atmospheres*, *123*(9), 4654–4673. https://doi.org/10.1002/2017JD028146

Van Doren, J. M., Watson, L. R., Davidovits, P., Worsnop, D. R., Zahniser, M. S., & Kolb, C. E. (1990). Temperature dependence of the uptake coefficients of nitric acid, hydrochloric acid and nitrogen oxide (N_2O_5) by water droplets. *The Journal of Physical Chemistry*, *94*(8), 3265–3269. https://doi.org/10.1021/j100371a009

Zhu, Y., Toon, O. B., Jensen, E. J., Bardeen, C. G., Mills, M. J., Tolbert, M. A., et al. (2020). Persisting volcanic ash particles impact stratospheric SO_2 lifetime and aerosol optical properties. *Nature Communications*, *11*(1), 4526. https://doi.org/10.1038/s41467-020-18352-5

References From the Supporting Information

Garcia, R. R., & Solomon, S. (1983). A numerical model of the zonally averaged dynamical and chemical structure of the middle atmosphere. *Journal of Geophysical Research*, *88*(C2), 1379–1400. https://doi.org/10.1029/JC088iC02p01379

Iacono, M. J., Delamere, J. S., Mlawer, E. J., Shephard, M. W., Clough, S. A., & Collins, W. D. (2008). Radiative forcing by long-lived greenhouse gases: Calculations with the AER radiative transfer models. *Journal of Geophysical Research*, *113*(D13), D13103. https://doi.org/10.1029/2008JD009944

Ivy, D. J., Solomon, S., Kinnison, D., Mills, M. J., Schmidt, A., & Neely, R. R., III. (2017). The influence of the Calbuco eruption on the 2015 Antarctic ozone hole in a fully coupled chemistry-climate model. *Geophysical Research Letters*, *44*(5), 2556–2561. https://doi.org/10.1002/2016GL071925

Kinnison, D. E., Brasseur, G. P., Walters, S., Garcia, R. R., Marsh, D. R., Sassi, F., et al. (2007). Sensitivity of chemical tracers to meteorological parameters in the MOZART-3 chemical transport model. *Journal of Geophysical Research*, *112*(D20), D20302. https://doi.org/10.1029/2006JD007879

Marsh, D. R., Mills, M. J., Kinnison, D. E., Lamarque, J.-F., Calvo, N., & Polvani, L. M. (2013). Climate change from 1850 to 2005 simulated in CESM1(WACCM). *Journal of Climate*, *26*(19), 7372–7391. https://doi.org/10.1175/JCLI-D-12-00558.1

Monier, E., & Weare, B. C. (2011). Climatology and trends in the forcing of the stratospheric zonal-mean flow. *Atmospheric Chemistry and Physics*, *11*(24), 12751–12771. https://doi.org/10.5194/acp-11-12751-2011

Solomon, S., Ivy, D. J., Kinnison, D., Mills, M. J., Neely, R. R., & Schmidt, A. (2016). Emergence of healing in the Antarctic ozone layer. *Science*, *353*(6296), 269–274. https://doi.org/10.1126/science.aae0061